Pharmacological Research 113 (2016) 216–227

Contents lists available at ScienceDirect

Pharmacological Research

journal homepage: www.elsevier.com/locate/yphrs

Signaling effects of sodium hydrosulfide in healthy donor peripheral blood mononuclear cells

André Sulen[a], Stein-Erik Gullaksen[a], Lucius Bader[c,d], David W. McClymont[e], Jørn Skavland[a], Sonia Gavasso[b,f], Bjørn T. Gjertsen[a,b,*]

[a] Centre for Cancer Biomarkers CCBIO, Department of Clinical Science, University of Bergen, Bergen, Norway
[b] Department of Internal Medicine, Hematology Section, Haukeland University Hospital, Bergen, Norway
[c] Department of Clinical Science, University of Bergen, Bergen, Norway
[d] Bergen Group of Epidemiology and Biomarkers in Rheumatic Disease (BEaBIRD), Department of Rheumatology, Haukeland University Hospital, Bergen, Norway
[e] Biotechnology Centre of Oslo, University of Oslo, Norway
[f] Neuroimmunology Lab, Department of Neurology, Haukeland University Hospital, Bergen, Norway

ARTICLE INFO

Article history:
Received 31 March 2016
Received in revised form 8 July 2016
Accepted 14 August 2016
Available online 16 August 2016

Chemical compounds studied in this article:
Sodium hydrosulfide (PubChem CID: 28015)
BIRB796 (PubChem CID: 156422)
PH-797804 (PubChem CID: 22049997)
Geldanamycin (PubChem CID: 5288382)
H-89 dihydrochloride (PubChem CID: 5702541)
Mibefradil dihydrochloride (PubChem CID: 60662)
BRL 50481 (PubChem CID: 2921148)
Chelerythrine chloride (PubChem CID: 72311)
BAPTA-AM (PubChem CID: 2293)

Keywords:
Hydrogen sulfide (H_2S)
Intracellular signaling
Phospho-specific antibodies
P38 mitogen activated protein kinase (MAPK)
Small molecule inhibitors
Calcium

ABSTRACT

Hydrogen sulfide (H_2S) is an endogenous gasotransmitter in human physiology and inflammatory disease, however, with limited knowledge of how signal transduction pathways are involved in immune cells. To examine the effects of sulfide on relevant intracellular signaling in human peripheral blood mononuclear cells (PBMCs), we stimulated healthy donor PBMCs with sodium hydrosulfide (NaHS, 1–1000 μM) to mimic H_2S stimulation, and analyzed phosphorylation of p38 mitogen activated protein kinase (MAPK) (pT180/pY182), NF-κB p65 (pS529), Akt (pS473) and CREB/ATF1 (pS133/pS63) with flow and mass cytometry. In contrast to transient effects in subsets of lymphocytes, classical monocytes demonstrated sustained phosphorylation of p38, Akt and CREB/ATF1. NaHS induced calcium dependent phosphorylation of p38, Akt and CREB, but not NF-κB, and the phosphorylation of Akt was partly dependent on p38, indicative of p38-Akt crosstalk. Attenuation of these effects by molecules targeting p38 and Hsp90 indicated Hsp90 as a possible target for H_2S-induced activation of p38. These results provide a description of a NaHS-induced signal transduction pathway in human primary immune cells that may have relevance for the role of sulfides in inflammation.

Abbreviations: H_2S, hydrogen sulfide; PBMCs, peripheral blood mononuclear cells; NaHS, sodium hydrosulfide; MAPK, mitogen activated protein kinase; NF-κB, nuclear factor kappa-light-chain-enhancer of activated B cells; CREB, cAMP response element-binding protein; ATF1, activating transcription factor 1; Hsp90, heat shock protein 90; PKC, protein kinase C; LPS, lipopolysaccharide; MFI, median (or mean) fluorescent intensity; EGTA, ethylene glycol-bis(β-aminoethyl ether)-N,N,N',N'-tetraacetic acid; BAPTA, 1,2-bis(o-aminophenoxy)ethane-*N*,*N*,*N*′,*N*′-tetraacetic acid; PMA, phorbol 12-myristate 13-acetate; GFP, green fluorescent protein.

* Corresponding author at: Centre for Cancer Biomarkers CCBIO, Department of Clinical Science, University of Bergen, 5020 Bergen, Norway.
E-mail address: bjorn.gjertsen@uib.no (B.T. Gjertsen).

http://dx.doi.org/10.1016/j.phrs.2016.08.018

1. Introduction

Hydrogen sulfide (H_2S) is a colorless malodorous gas that has received a substantial interest as an important gasotransmitter in regulation of inflammation [1–3]. H_2S is produced endogenously through the transsulfuration or 3-mercaptopyruvate sulfurtransferase/H_2S pathway [4–7], and the concentration of free H_2S in plasma is below 1 μM [8,9]. The concentration of endogenous H_2S is increased during sepsis, hemorrhagic shock and in cardiovascular disease [10–12]. Higher levels of H_2S are also measured in synovial fluid of chronically inflamed joints in rheumatoid arthritis patients [13,14]. As an exogenous source, inhalation of higher than ambient concentrations of H_2S is estimated to lead to an increase in plasma sulfide concentration [15]. Further, H_2S-releasing drugs are also developed and used for their anti-inflammatory properties in treatment of gastrointestinal disorders [16]. However, the role of H_2S as a possible mediator during inflammation remains elusive, with disparate inflammatory effects attributed to this gasotransmitter [10,11,13,14,17–21].

The transcription factor NF-κB is considered a key regulator of inflammation [22,23], and stimulation of the tumor necrosis factor receptors (TNFRs) or Toll like receptors (TLRs) typically activate both NF-κB p65 and p38 [24,25]. The p38 MAPK signaling pathway is involved in several aspects of inflammation, such as production of both pro- and anti-inflammatory cytokines, prostaglandin synthesis and inducible nitric oxide synthase (iNOS) production [26–30]. H_2S is known to modulate NF-κB activity through sulfhydration [31,32], and to increase phosphorylation of p38 in beta cells [33], vascular smooth muscle cells [34], endothelial cells [35] and glioma cells [36] but decrease phosphorylation in neutrophils [37]. Activation of protein kinase C (PKC) or the calcium/calmodulin dependent signaling cascade can both lead to p38 phosphorylation [30,38–40]. Preconditioning of cardiomyocytes with H_2S leads to cardioprotection and PKC activation, and this cardioprotection is attenuated by the PKC inhibitor chelerythrine [41]. Activation of conventional PKC isoforms is dependent on calcium [42], and H_2S is also reported to influence calcium homeostasis in excitable cells [41,43]. Whether H_2S activates p38 in PBMCs and if PKC or calmodulin dependent signaling is involved is not known.

Crosstalk between p38 and the proliferative Akt pathway during stimulation with lipopolysaccharide (LPS) or formyl-methionyl-leucyl-phenylalanine (fMLP) has been described to take place via the MAPK-activated protein kinases MK2/3 in macrophages [44] and neutrophils [45], respectively. H_2S treatment alone increases phosphorylation of Akt (S473) in rat myocardium tissue [46], pancreatic acinar cells [47] and endothelial cells [48], but only in endothelial cells have H_2S-induced Akt phosphorylation been shown to be p38 dependent, indicating p38-Akt crosstalk [48]. Akt plays a role in polarization of macrophages differentiation [49], but whether p38-Akt crosstalk takes place in primary monocytes during treatment with H_2S is, however, unknown. The use of comprehensive high dimensional single cell signaling assessment to describe the effects of H_2S on signal transduction in primary immune cells is so far in its infancy [50], and conventional flow cytometry and mass cytometry is a particular powerful technique suitable for delineating effects of small molecular inhibitors or activators in complex mixtures of blood cells [51–53]. To better understand how this gasotransmitter influence immune cells, we investigated how sodium hydrosulfide affects p38 MAP kinase and NF-κB intracellular signaling systems of PBMCs.

2. Materials and methods

2.1. Chemicals

Sodium hydrosulfide (NaHS) was acquired from Sigma-Aldrich (St. Louis, MO, USA), and a fresh stock was prepared prior to each experiment by dissolving it in saline at 0.2 M. The molecules ryanodine, 2-aminoethoxydi-phenyl borate (2-APB), W-7, KN-93, geldanamycin and ethylene glycol-bis(2-aminoethyl)-*N,N,N,N*-tetraacetic acid (EGTA) were purchased from Sigma-Aldrich. BAPTA-AM was purchased from Thermo Fisher Scientific (Waltman, MA, USA). The molecules RO318220, GÖ6976, LY333531, chelerythrine and PKC-412 were purchased from Santa Cruz (Dallas, TX, USA). BIRB796 and PH-797804 were acquired from Selleckchem (Houston, TX, USA). All molecules except EGTA were dissolved in DMSO. EGTA was dissolved in double distilled water (ddH_20) adjusted to pH 7.5. Paraformaldehyde (16%) was purchased from Thermo Fisher Scientific. Molecules used in the automated screen were selected from libraries from Selleckchem, Enzo Life Sciences (Farmingdale, NY, USA), Tocris Bioscience (Bristol, UK) or Sigma (details in Supplemental Table S2).

2.2. Culturing of THP-1 and Jurkat cells and isolation of PBMCs

The T-cell leukemia cell line Jurkat (Clone E6-1) and the myeloid cell line THP-1 were purchased from ATCC (American Type Culture Collection, Manassas, VA, USA). Dr. Vibeke Andresen (University of Bergen, Norway) kindly provided the NF-κB/Jurkat/GFP™ Transcriptional Reporter Cell Line (System Biosciences, Palo Alto, CA, USA). All cells were cultured in Roswell Park Memorial Institute (RPMI)-1640 medium (Sigma-Aldrich, Inc. St. Louis, MO, USA) with 10% heat-inactivated Fetal Bovine Serum (PAA Laboratories GmbH, Austria), 1% L-glutamine (Sigma-Aldrich) and 1% Penicillin/Streptomycin (Sigma-Aldrich). Cells were cultured at 5% CO_2 humidified atmosphere at 37 °C. PBMCs were acquired from random healthy blood donors from the Department of Immunology and Transfusion Medicine, Haukeland University Hospital, Bergen, Norway. The local research ethics committee at Haukeland University Hospital approved the study (Regionale komiteer for medisinsk og helsefaglig forskningsetikk, REK), and the donors provided informed consent. Blood was collected in accordance with the Helsinki Declaration. Blood collected in EDTA tubes was diluted in saline (1:2) prior to density gradient separation (Lymphoprep™, Stemcell Technologies). PBMCs were isolated and washed two times in sterile saline prior to resuspension at 0.5×10^6 cells/ml in complete RPMI medium. PBMCs were kept in an incubator at 5% CO_2 humidified atmosphere at 37 °C for at least 60 min prior to experiments.

2.3. In vitro treatment of cells

For phospho flow cytometry experiments, PBMCs or cell lines were transferred to polypropylene flow cytometry tubes purchased from Sarstedt (Germany). After treatment of cells for the desired treatment time, cells were fixed by adding 16% paraformaldehyde to a final concentration of 4%. The fixation process was carried out at room temperature for 15 min prior to washing with saline. Cells were centrifuged at 1200 rpm for 5 min and subsequently resuspended in ice-cold methanol. Cells were immediately stained for flow cytometry or stored at −80 °C until staining. For mass cytom-

etry analysis, cells were treated in accordance with protocols from Fluidigm.

2.4. Phospho specific flow cytometry

In order to reduce antibody consumption and to achieve accurate staining, samples were fluorescently barcoded prior to antibody staining [54]. PBMCs were barcoded with the amine-reactive fluorescent dyes Pacific Blue and Pacific Orange while THP-1 cells were barcoded with Alexa568 and Pacific Blue (all from Thermo Fisher Scientific). Staining of cells with phospho specific antibodies and antibodies for immunophenotyping was carried out as previously described [50,55]. The cells were stained with monocyte surface marker CD163 PE (Clone MAC2-158, Trillium Diagnostics), T-cell marker CD5 PerCP-Cy5.5 (Clone L17F12, BD), Anti p38 MAPK (pT180/pY182, clone 36/p38, BD), Anti-CREB/ATF1 (pS133/pS63, clone J151-21, BD) or Anti-Akt (pS473, clone M89-61). After antibody staining the samples were analyzed on a FACS Fortessa flow cytometer (BD). For the high throughput small molecule inhibitor screen the standard phosphoflow method was fully automated in 384-well format using a Microlab Star liquid handling robot (Hamilton).

2.5. Mass cytometry analysis

Stimulated cells were barcoded using the 20-plex barcoding kit (Fluidigm) and stained with a single panel of 19 mass-tagged antibodies (Supplemental Table S1), in accordance with cell staining protocols (Fluidigm). Cells were analyzed on a Helios mass cytometer (Fluidigm) at approx. 400 events/s. An automated barcode deconvolution algorithm was used to identify barcoded samples and to remove cell doublets. Unsupervised multiparameter viSNE analysis was used to identify cellular subsets of PBMCs [56]. All antibodies used for mass cytometry was purchased from Fluidigm and are listed in Supplemental Table 1.

2.6. Cell death assay

Viability of PBMCs treated with different concentrations of NaHS was determined by staining the cells with Annexin V Alexa® 647 conjugate (BD) and analysis of the cells with flow cytometry. Viability of Jurkat cells was determined with a Colony-Forming Cell Assay using MethoCult™ H4434 Classic (Stemcell™ Technologies).

2.7. ATP measurements

Concentrations of ATP in PBMCs were determined with the CellTiter-Glo® Luminescent Cell Viability Assay (Promega, Madison, WI, USA). The luminescence was measured with the Infinite® M200 reader (Tecan Trading AG, Switzerland).

2.8. Statistical analysis

A two-tailed Student's t-test was carried out in Prism 6 to compare phosphorylation levels between control groups and treatment groups in the different cell types. The significance level was set to 0.05.

3. Results

3.1. NaHS induces phosphorylation of p38 (T180/Y182) in peripheral blood mononuclear cells

Stimulation of PBMCs with NaHS followed by evaluation of phosphorylated p38 with western blotting and phospho specific flow cytometry showed a concentration-dependent increase in p-p38 (Fig. 1a, b). Correlation between quantitated bands from the western blot with mean fluorescent intensities (MFI) indicates high specificity for the flow cytometry assay (Fig. 1c). To determine the optimal stimulation time, PBMCs were stimulated with NaHS (1 mM) for various treatment times and evaluated for p-p38 (Fig. 1d). Phosphorylation peaked after 5–10 min, and the phosphorylation of p-p38 was sustained and transient in monocytes and T-cells, respectively. The phosphorylation remained sustained in monocytes for 4 h (longest treatment time tested, data not shown). With the optimal treatment time for signaling, PBMCs were stimulated with increasing concentrations of NaHS (1–1000 μM, 10 min) and evaluated for p-p38 (Fig. 1e, f). NaHS displayed an EC_{50} of 183 μM (95% CI (53, 642)) in T-cells and 95 μM (95% CI (77, 117)) in monocytes (Fig. 1f). For the remaining signal transduction experiments in the study, cells were stimulated with 1 mM NaHS for 10 min unless otherwise stated. To investigate how NaHS effects p-p38 in the different types of monocytes and lymphocytes present in PBMCs, a mass cytometry panel counting 19 antibodies was developed for immune phenotyping of PBMCs and evaluation of signal transduction in these cells during treatments. The complex immune phenotypic data was analyzed with the unsupervised viSNE analysis, and manually divided into different subsets of lymphoid and myeloid cells (Supplemental Fig. S3). Phosphorylation of p38 was observed to increase in CD4 T-cells, CD8 T-cells, B-cells, natural killer (NK) cells, basophils, and both classical and non-classical monocytes after stimulation with NaHS (Fig. 1g). The phosphorylation remained high after 60 min in classical monocytes, but not in non-classical monocytes. CD123+ dendritic cells (DCs) did not display a change in p-p38 during stimulation with NaHS. Further, NaHS was found to induce substantial cell death at 1 mM but not at 0.1 mM, as determined in an Annexin V assay (Fig. 1h). Given that H_2S is a potent inhibitor of cytochrome-c oxidase and mitochondrial respiration [57], ATP was measured in PBMCs treated *in vitro* with concentrations shown to phosphorylate p38 (Fig. 1i). No significant changes were observed when compared to vehicle treated cells.

3.2. Phosphorylation of p38 (T180/Y182) by NaHS takes place independently of extracellular calcium but is dependent on intracellular calcium in PBMCs

Given that H_2S is reported to influence calcium homeostasis in various cell types, we therefore sought to investigate if the observed NaHS-induced phosphorylation of p38 in PBMCs could be dependent on calcium. When evaluating the role of extracellular calcium, preincubation with EGTA did not attenuate the increase in p-p38 induced by any concentration of NaHS compared to cells not pre-incubated with EGTA (Fig. 2a). Treating PBMCs with EGTA and ionomycin (0.5 μg/ml, 10 min) validated the effect of calcium chelation by EGTA on p-p38 (Fig. 2b). Using a different chelator of extracellular calcium (BAPTA) in combination with NaHS gave the same results (Fig. 2c). When evaluating the role of intracellular calcium, preincubation with BAPTA-AM did result in complete attenuation of NaHS-induced p38 phosphorylation as compared to cells where calcium was not chelated (Fig. 2d). Repeating the experiments with BAPTA and BAPTA-AM on PBMCs from additional blood donors confirmed these results (Fig. 2e).

3.3. Pharmacological inhibition of IP_3R, RyR, calmodulin, CaMKII or PKC do not inhibit NaHS-induced modulation of p38 phosphorylation (T180/Y182) in PBMCs

The classical regulator of calcium release from the endoplasmatic reticulum (ER) during PKC activation is inositol 1,4,5 trisphosphate receptor (IP_3R) [58]. Calcium release from ER via

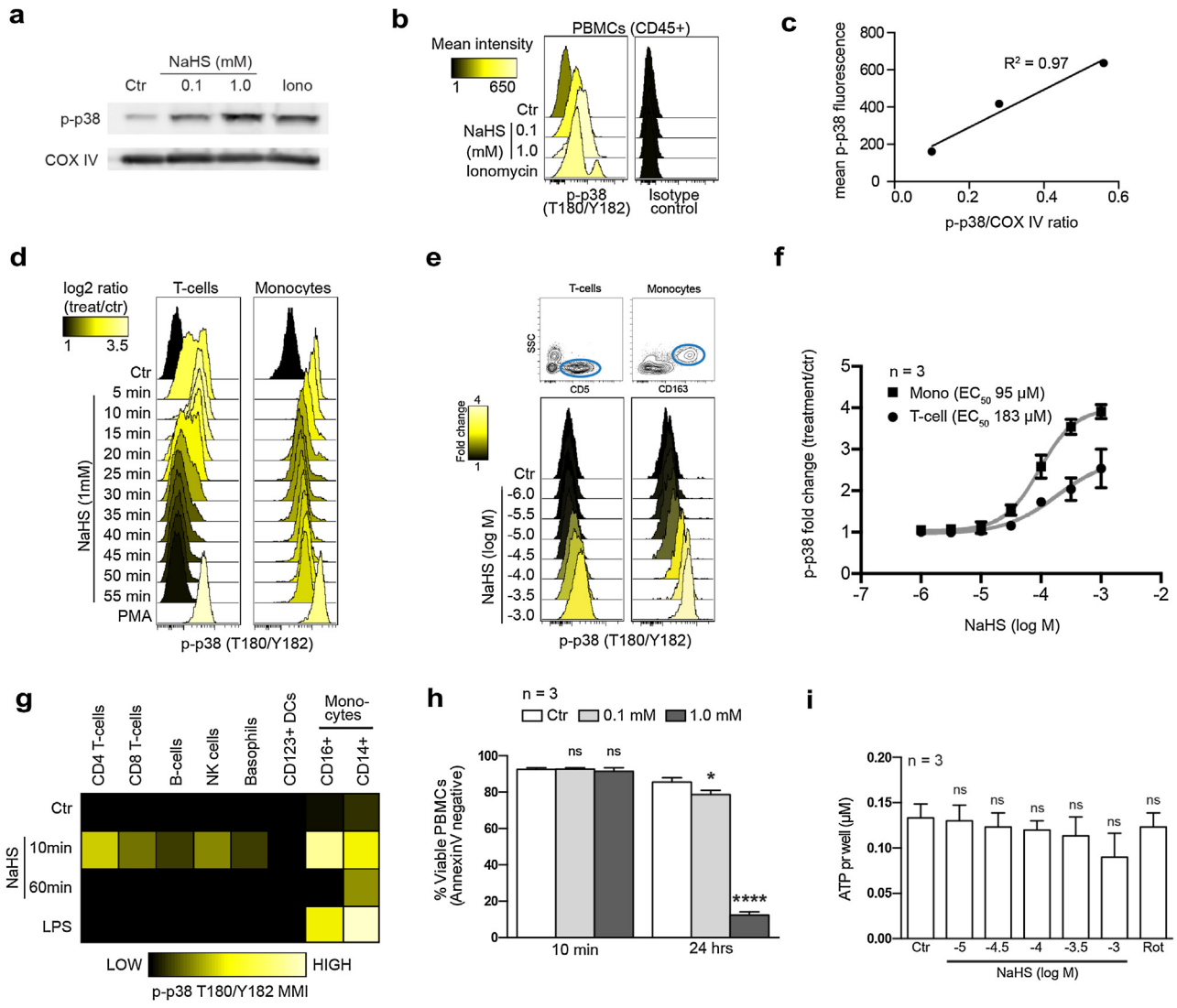

Fig. 1. *In vitro* treatment of PBMCs with sodium hydrosulfide induces phosphorylation of p38 (T180/Y182). (a) Cropped western blots of lysates from PBMCs treated with NaHS (10 min) or ionomycin (0.5 μg/ml, 10 min). Uncropped images are available in Supplemental Figs. S1 and S2 . (b) Histogram overlay displays p-p38 T180/Y182 or isotype control stained CD45+ PBMCs stimulated with NaHS (10 min) or ionomycin (0.5 μg/ml, 10 min). (c) Dot plot comparing PBMC p-p38 mean fluorescent intensity with p-p38/COX IV ratios. Solid line represents linear regression line. (d, e) Histogram overlays display ratio (treated/ctr) of p-p38 T180/Y182 in T-cells (CD5 +) and monocytes (CD163 +) stimulated with 1 mM NaHS for increasing treatment times (5–55 min) (d) or increasing concentrations of NaHS (1–1000 μM) for 10 min (e). (f) PBMCs from healthy donors (n = 3) were stimulated with NaHS (1–1000 μM, 10 min), and p-p38 MFI determined by flow cytometry was used to make concentration-response curves (mean ± SD). (g) Heat map displaying median metal intensity (MMI) of p-p38 (T180/Y182) in subsets of PBMCs identified in Supplemental Fig. S3. The cells were treated with NaHS (1 mM, 10 or 60 min) or LPS (1.0 μg/ml, 10 min). (h) Plot displaying percentage Annexin V negative cells (mean ± SD) in PBMCs treated with NaHS (0.1 or 1.0 mM, 10 min or 24 h) or vehicle. Student's *t*-tests were conducted to compare treated groups and control (*$p \leq 0.05$, ****$p \leq 0.0001$, ns $p > 0.05$). (i) Plot displaying ATP concentrations (mean ± SD) determined with CellTiter-Glo® after treating PBMCs with NaHS (10–1000 μM) or rotenone (1 μM) for 10 min. Student's *t*-tests were conducted to compare treated groups and control (ns $p > 0.05$).

IP_3R is activated by the ligand IP_3, a molecule produced by phospholipase C (PLC) through hydrolysis of phosphatidylinositol 4,5-bisphosphate (PIP_2) during receptor activation [58]. In order to assess whether the observed signaling effects of NaHS were due to calcium mobilization via IP_3Rs, PBMCs were pre-incubated with the IP_3R antagonist 2-aminoethoxydiphenyl borate (2-APB) before stimulation with NaHS, and evaluated for p-p38. This did not prevent increased p-p38 induced by NaHS (Fig. 3a). Intracellular calcium release in immune cells is also suggested mediated by the ryanodine receptors (RyRs) [59]. While RyRs are highly expressed in brain tissue and in skeletal and cardiac muscle tissue, the expression in PBMCs are limited to only some subsets of cells and at low levels [59]. To assess whether NaHS-induced elevated p-p38 could be due to calcium mobilization via RyRs, PBMCs were preincubated with antagonistic concentrations of ryanodine before stimulation with NaHS, and evaluated for p-p38. Antagonistic concentrations of ryanodine had no observed effect on the phosphorylation of p38 induced by NaHS (Fig. 3c). The plant alkaloid ryanodine functions as an RyR agonist at low concentrations (nM) by locking the receptor in an open state, while it functions as an RyR antagonist at higher concentrations (μM) [60]. Incubating PBMCs with agonistic concentrations of ryanodine alone (1–100 nM, 10 min) did not result in any change in p-p38 (data not shown).

To assess whether the inhibition of calmodulin or Ca^{2+}/calmodulin-dependent protein kinase II (CaMKII) could attenuate the increase in p-p38, PBMCs were preincubated with the calmodulin inhibitor W-7 or the CaMKII inhibitor KN93 prior to stimulation with NaHS. None of the inhibitors caused a substantial attenuation of the p38 phosphorylation induced by NaHS (Fig. 3b). In accordance with this, repeating these experiments with the

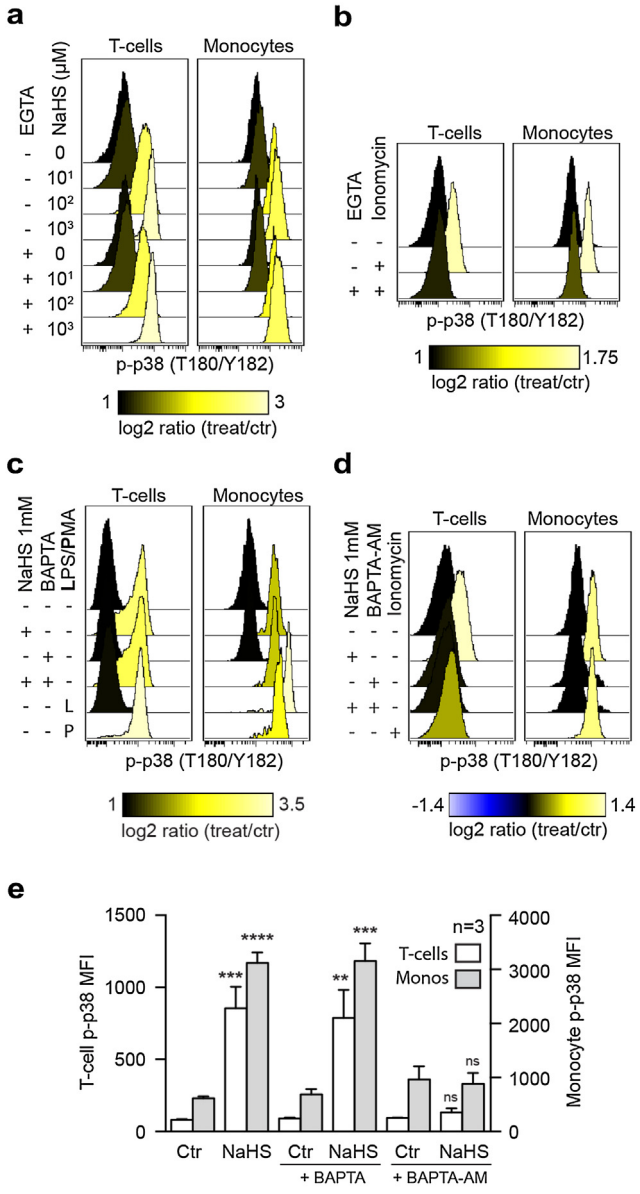

Fig. 2. Phosphorylation of p38 (T180/Y182) during *in vitro* treatment of PBMCs with sodium hydrosulfide is independent of extracellular calcium but dependent on intracellular calcium. (a-d) Histogram overlays display median ratio (treatment/ctr) of p-p38 in T-cells and monocytes. (a) Cells were treated with NaHS (10, 100 or 1000 μM for 10 min) or left untreated, after preincubation with or without EGTA (2 mM, 15 min). (b) PBMCs were stimulated with ionomycin (0.5 μg/ml, 10 min) or left untreated, after preincubation with or without EGTA (2 mM, 15 min). (c) PBMCs were stimulated with NaHS (10 min) or left untreated, after preincubation with or without BAPTA (2 mM, 15 min). (d) PBMCs were stimulated with NaHS (10 min) or left untreated, after preincubation with or without BAPTA-AM (20 μM, 60 min). (e) Plot displaying p-p38 MFIs (mean ± SD) of T-cells and monocytes in treated (NaHS, 1 mM, 10 min) and untreated samples, with or without preincubation with BAPTA (2 mM, 15 min) or BAPTA-AM (20 μM, 60 min). Student's *t*-tests were conducted to compare p-p38 in treated groups (NaHS) and their respective controls (**$p \leq 0.01$, ***$p \leq 0.001$, ****$p \leq 0.0001$, ns $p > 0.05$).

monocytic cell line THP-1 gave similar results (Supplemental Fig. S4). To investigate whether pharmacological inhibition of PKC could attenuate the increase in p-p38, PBMCs were preincubated with GÖ6976, LY333531 or chelerythrine prior to stimulation with NaHS. GÖ6976 and LY333531 did not attenuate the NaHS-induced effect on p-p38 (Fig. 3d). Chelerythrine alone did induce a large phosphorylation of p38, and after preincubating with chelerythrine there was no observable difference in p-p38 between control and NaHS treated cells. Similar effects by GÖ6976 and chelerythrine on

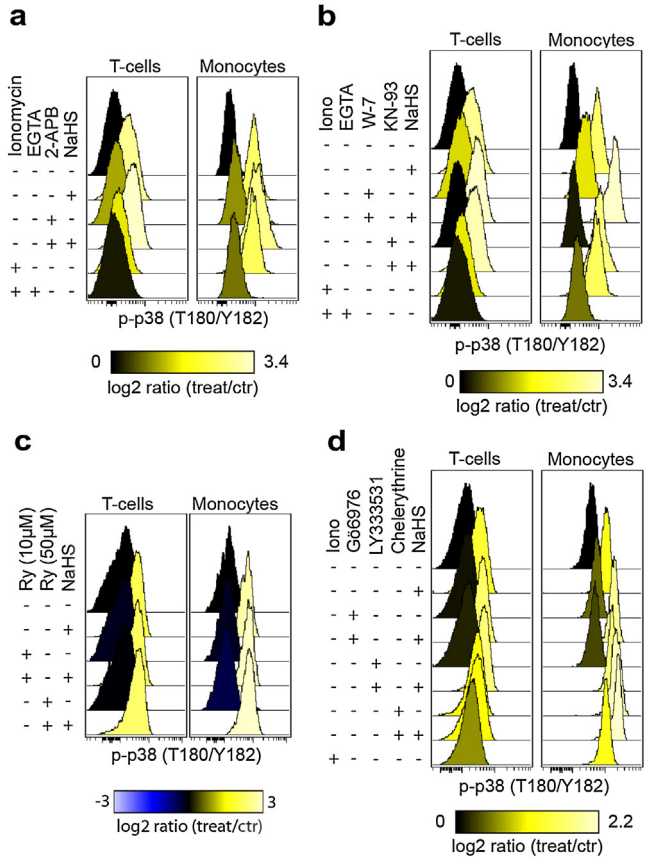

Fig. 3. Phosphorylation of p38 during *in vitro* treatment of PBMCs with sodium hydrosulfide is independent of inhibition of IP3R, RyR, calmodulin, CaMKII and PKC. (a-d) Histogram overlays display median ratio (treatment/ctr) of p-p38 in T-cells and monocytes. PBMCs were stimulated with NaHS (1 mM, 10 min) or left untreated, after preincubation for 15 min with or without (a) 2-APB (300 μM), (b) W-7 (50 μM) or KN-93 (5 μM), (c) ryanodine, and (d) GÖ6976 (3 μM), LY333531 (7.5 μM) or chelerythrine (3 μM).

NaHS-induced p-p38 were observed in THP-1 cells (Supplemental Fig. S4). Incubating THP-1 cells with two additional PKC inhibitors (PKC412 and RO318220) prior to stimulation with NaHS did not prevent p-p38 induction (Supplemental Fig. S4).

3.4. Inhibitors targeting p38 and Hsp90 attenuate the increase in phosphorylation of p38 (T180/Y182) induced by NaHS

In order to further elucidate how p38 is phosphorylated by NaHS, Jurkat cells were chosen as a suitable model in which to carry out an automated high throughput phosphoflow screen with a library of relevant small molecule inhibitors to evaluate how these molecules influence the phosphorylation induced by NaHS (Fig. 4a). Jurkat cells treated with 0.1 or 1.0 mM NaHS did not show significant less viability compared to vehicle treated cells (determined with a colony-forming assay, data not shown). Of the 59 compounds tested (Supplemental Table S2), two p38 inhibitors (BIRB796 and PH-797804) and the Hsp90 inhibitor geldanamycin significantly attenuated the effect of NaHS on p-p38 (grey box in Fig. 4a). In addition, three compounds known to target phosphodiesterases (PDEs), protein kinase A (PKA) and T-type Ca^{2+} channels appeared to slightly attenuate the effect of NaHS, however not significantly. The effect of BIRB796, PH-797804 and geldanamycin on p38 phosphorylation induced by NaHS was further validated in primary PBMCs (Fig. 4b–d). Pre-incubation with geldanamycin attenuated the effect of NaHS by inducing phosphorylation of p38 alone in both PBMCs and the Jurkat cells (Fig. 4d and Supplemental Fig. S6).

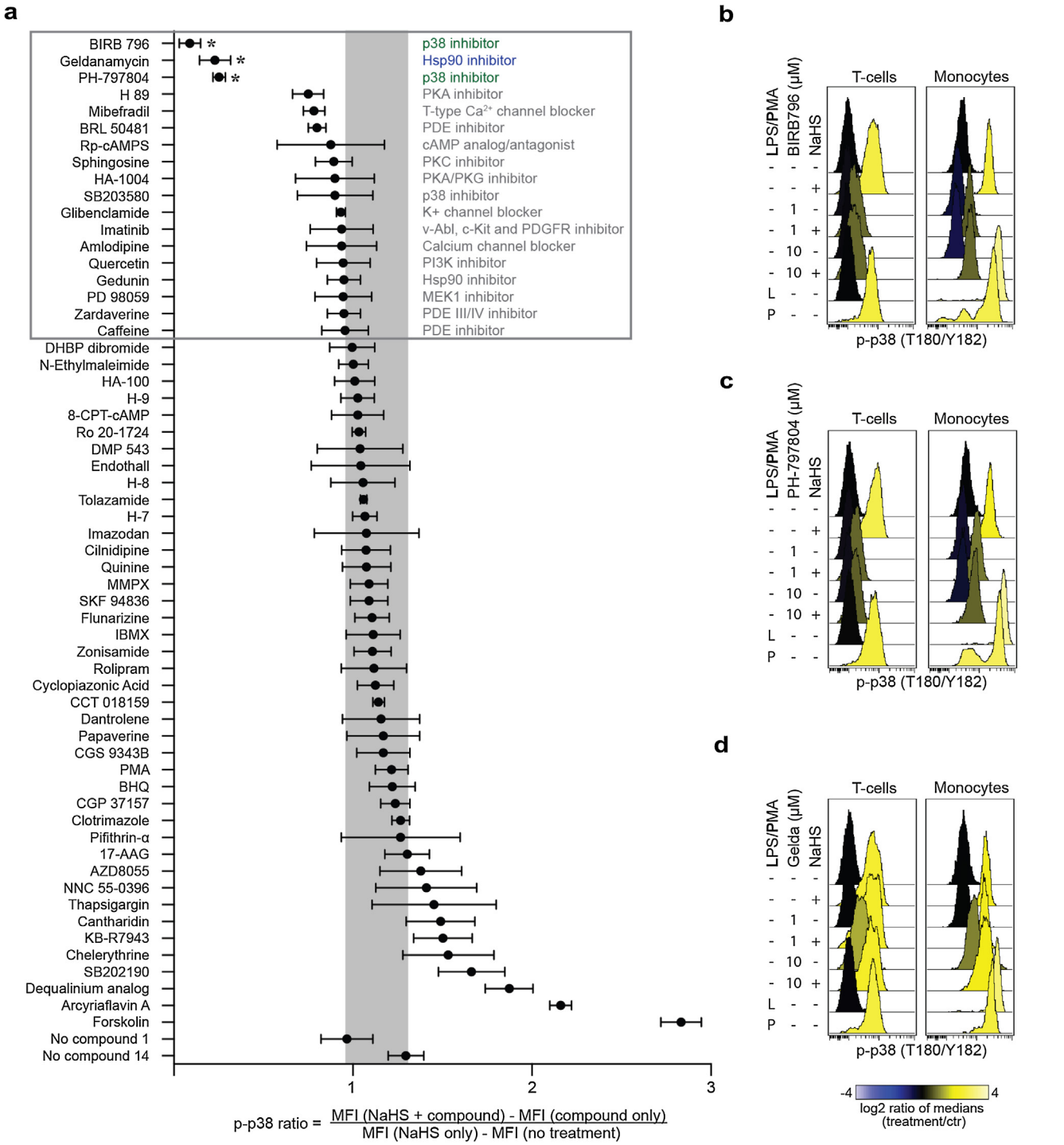

Fig. 4. Inhibitors of p38 and Hsp90 attenuate increase in phosphorylation of p38 induced by NaHS. (a) Jurkat cells were incubated with small molecule inhibitors (10 μM) in 25 min prior to stimulation with NaHS (1 mM, 2.5 min). Plot displays the ratio between p38 phosphorylation induced by NaHS when preincubating with and without compounds (*$p < 0.05$, *t*-test (compared to "No compound 1")). The grey area represents the expected variation in the assay without compounds (determined by 14 replicates without compounds, see Supplemental Figs. S5 and S6 for quality control data). All compounds were tested in triplicates. (b-d) Histogram overlays display effect of inhibitors targeting p38 and Hsp90 (1 and 10 μM, 25 min) on phosphorylation of p38 induced by NaHS (1 mM, 10 min) in PBMCs.

3.5. *NaHS induces calcium-dependent phosphorylation of Akt that is partly dependent on p38 in PBMCs*

To investigate if Akt is phosphorylated during treatment of PBMCs with H_2S, blood cells were stimulated with NaHS (1 mM) for treatment times up to an hour and evaluated for p-Akt (S473) (Fig. 5a). Similar to p38, Akt was phosphorylated in a transient and sustained manner in T-cells and monocytes, respectively (Fig. 5a). To investigate if this observed phosphorylation of Akt could be due to crosstalk from the p38 signaling pathway, PBMCs were preincubated with the indirectly ATP-competitive p38 inhibitor BIRB796, stimulated with NaHS (1 mM, 10 min) and the phosphorylation level of Akt was determined by flow cytometry. Inhibition of p38 did significantly attenuate the induction of p-Akt by NaHS in monocytes (*t*-test, $p < 0.05$), however, not significantly in T-cells (Fig. 5b-c). Inhibition of p38 also significantly attenuated the

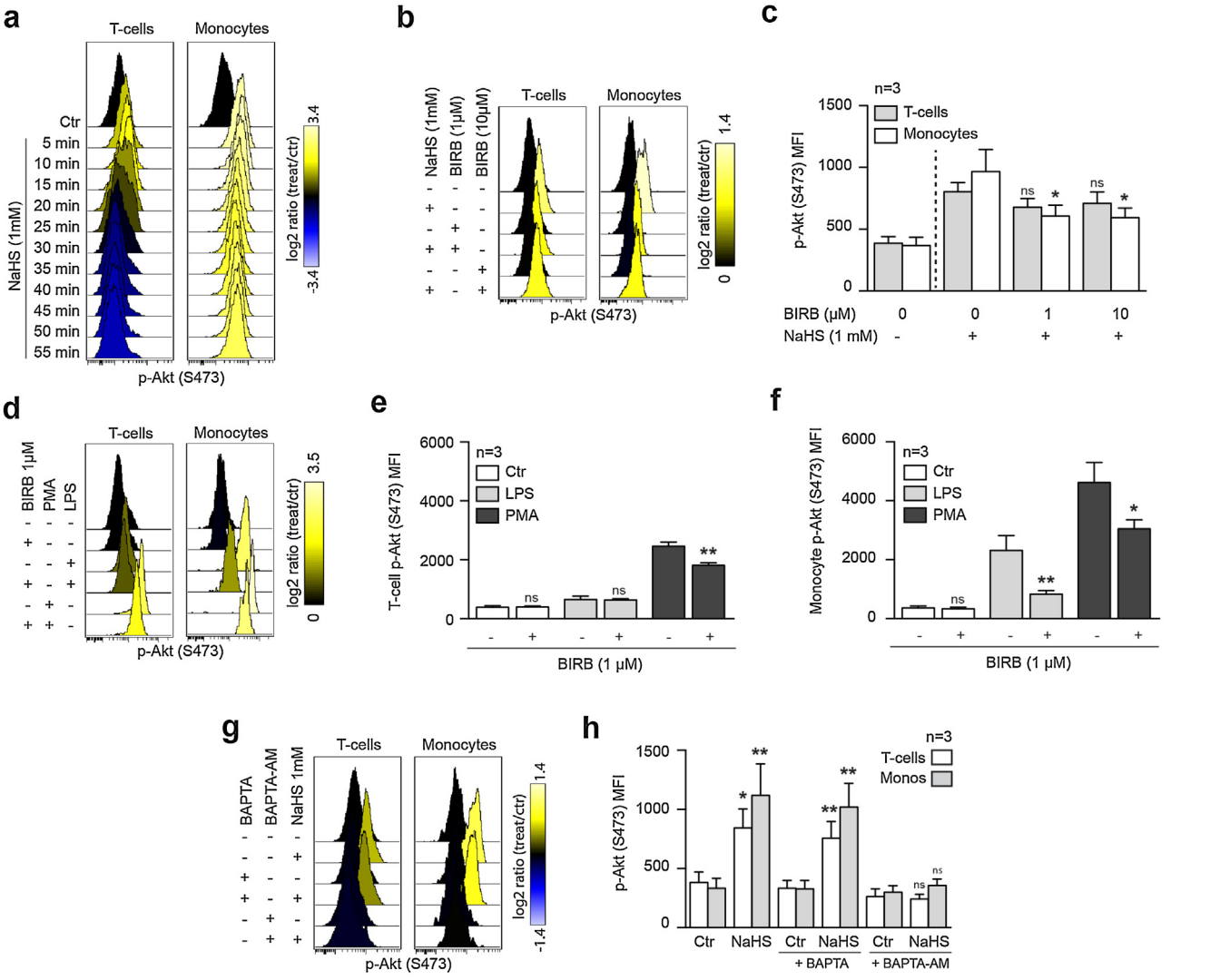

Fig. 5. NaHS induces phosphorylation of Akt that is partly dependent on p38 and dependent on intracellular calcium in PBMCs (a) Histogram overlay displays median ratio (treatment/ctr) of p-Akt in T-cells and monocytes stimulated with NaHS (1 mM) for treatment times up to 55 min. Vehicle treated cells were used as control. (b) Histogram overlay displays median ratio (treatment/ctr) of p-Akt in T-cells and monocytes stimulated with NaHS (10 min) or left untreated, after preincubation with or without BIRB796 (25 min). (c) Plot displaying p-Akt MFIs (mean ± SD) of T-cells and monocytes in treated (NaHS, 10 min) and untreated samples, with or without preincubation with BIRB796 (25 min). Student's *t*-tests were conducted to compare p-Akt in combination groups (NaHS + BIRB796) with groups only treated with NaHS (*$p \leq 0.05$, ns $p > 0.05$). (d) Histogram overlay displays median ratio (treatment/ctr) of p-Akt in T-cells and monocytes stimulated with PMA (1 µg/ml, 15 min), LPS (1 µg/ml, 15 min) or left untreated, after preincubation with or without BIRB796 (25 min). (e-f) Plots displaying p-Akt MFIs (mean ± SD) of (**e**) T-cells and (**f**) monocytes in treated (LPS or PMA) and untreated samples, with or without preincubation with BIRB796 (25 min). Student's t-tests were conducted to compare p-Akt in BIRB796 groups with their respective controls (*$p \leq 0.05$, **$p \leq 0.01$, ns $p > 0.05$). (g) Histogram overlay displays median ratio (treatment/ctr) of p-Akt in T-cells and monocytes stimulated with NaHS (10 min) or left untreated, after preincubation with or without BAPTA (2 mM, 15 min) or BAPTA-AM (20 µM, 60 min). (h) Plot displaying p-Akt median fluorescent intensities of T-cells and monocytes in treated (NaHS, 1 mM, 10 min) and untreated samples, with or without preincubation with BAPTA (2 mM, 15 min) or BAPTA-AM (20 µM, 60 min). Student's *t*-tests were conducted to compare p-Akt in treated groups (NaHS) with their respective control groups (*$p \leq 0.05$, **$p \leq 0.01$, ns $p > 0.05$).

induction of p-Akt by LPS in monocytes (*t*-test, $p < 0.01$) and by PMA in both cell types (*t*-test, $p < 0.05$) (Fig. 5d–f). Since intracellular calcium chelation completely attenuated the NaHS-induced phosphorylation of p38, this was also investigated for p-Akt. Intracellular calcium chelation resulted in a complete inhibition of increase in p-Akt induced by NaHS (Fig. 5g-h).

3.6. NaHS induces cAMP responsive element (CRE)-binding transcription factor phosphorylation that is dependent on p38 and intracellular calcium in PBMCs

The kinase p38 is known to form a signaling pathway involving CRE-binding transcription factors [30]. To investigate the kinetics of CREB/ATF1 phosphorylation during stimulation with NaHS, PBMCs were stimulated with NaHS (1 mM) for treatment times up to an hour and evaluated for p-CREB/ATF-1 with flow cytometry (Fig. 6a). Similar to p38 and Akt, CREB is phosphorylated in a transient and sustained manner in T-cells and monocytes, respectively (Fig. 6a). For testing whether CREB/ATF-1 is downstream of p38, inhibition of p38 did significantly attenuate the NaHS-induced phosphorylation of CREB/ATF1 in monocytes and T-cells (t-test, $p < 0.001$) (Fig. 6b-c). Inhibition of p38 also significantly attenuated the induction of p-CREB/ATF-1 by LPS in monocytes (t-test, $p < 0.01$), but not by PMA in any cell types (Fig. 6d–f). Intracellular calcium chelation with BAPTA-AM resulted in a complete inhibition of the increase in monocyte p-CREB/ATF-1 induced by NaHS (Fig. 6g-h). BAPTA-AM alone increased the phosphorylation of CREB/ATF1 in T-cells, but no significant additional increase was observed when combined with NaHS (Fig. 6g-h).

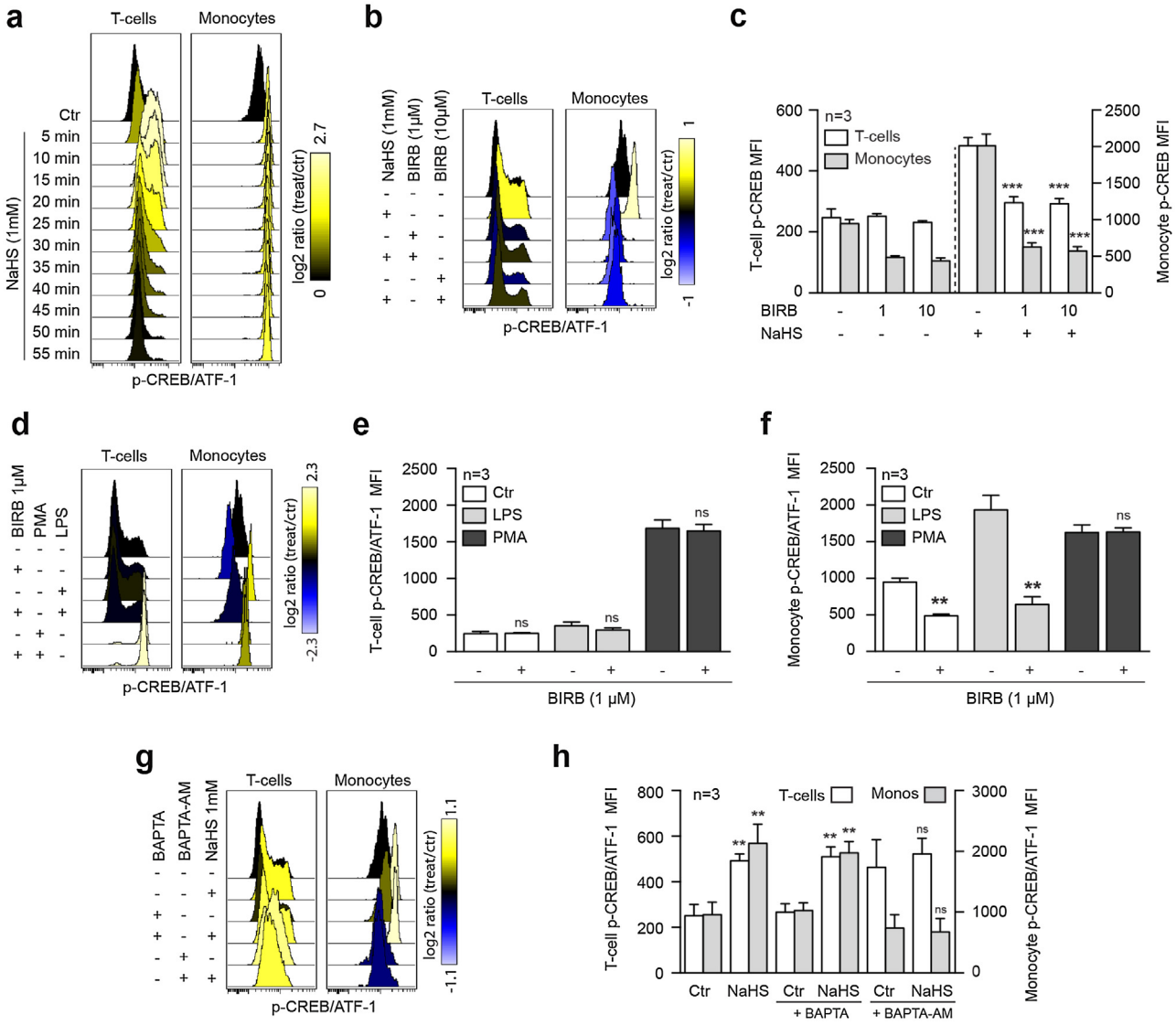

Fig. 6. NaHS induces phosphorylation of CREB/ATF-1 that is dependent on p38 and intracellular calcium in PBMCs. (a) Histogram overlay displays median ratio (treatment/ctr) of p-CREB/ATF-1 in T-cells and monocytes stimulated with NaHS (1 mM) for treatment times up to 55 min. Vehicle treated cells were used as control. (b) Histogram overlay displays median ratio (treatment/ctr) of p-CREB/ATF-1 in T-cells and monocytes stimulated with NaHS (10 min) or left untreated, after preincubation with or without BIRB796 (25 min). (c) Plot displaying p-CREB/ATF-1 MFIs (mean ± SD) of T-cells and monocytes in treated (NaHS, 1 mM, 10 min) and untreated samples, with or without preincubation with BIRB796 (1 or 10 μM, 25 min). Student's *t*-tests were conducted to compare p-CREB/ATF-1 in combination groups (NaHS + BIRB796) with groups only treated with NaHS (***$p \leq 0.001$). (d) Histogram overlay displays median ratio (treatment/ctr) of p-CREB/ATF-1 in T-cells and monocytes stimulated with PMA (1 μg/ml, 15 min), LPS (1 μg/ml, 15 min) or left untreated, after preincubation with or without BIRB796 (25 min). (e-f) Plots displaying p-CREB/ATF-1 MFIs (mean ± SD) of (e) T-cells and (f) monocytes in treated (LPS or PMA) and untreated samples, with or without preincubation with BIRB796 (25 min). Student's *t*-tests were conducted to compare p-CREB/ATF-1 in BIRB796 groups with their respective control groups (**$p \leq 0.01$, ns $p > 0.05$). (g) Histogram overlay displays median ratio (treatment/ctr) of p-CREB/ATF-1 in T-cells and monocytes stimulated with NaHS (10 min) or left untreated, after preincubation with or without BAPTA (2 mM, 15 min) or BAPTA-AM (20 μM, 60 min). (h) Plot displaying p-CREB/ATF-1 median fluorescent intensities of T-cells and monocytes in treated (NaHS, 1 mM, 10 min) and untreated samples, with or without preincubation with BAPTA (2 mM, 15 min) or BAPTA-AM (20 μM, 60 min). Student's *t*-tests were conducted to compare p-CREB/ATF-1 in treated groups (NaHS) with their respective control groups (**$p \leq 0.01$, ns $p > 0.05$).

3.7. *NaHS does not activate NF-κB*

In order to investigate how H_2S influences NF-κB in PBMCs, these cells were stimulated with NaHS (1 mM), TNFα (20 ng/ml) or LPS (1 μg/ml) for ten minutes and evaluated for p-p38 and p-NF-κB (S529) with flow cytometry. Stimulation with TNF and LPS induced phosphorylation of both proteins in the expected cell types (Fig. 7a). Stimulation with NaHS induced phosphorylation of p38, but not NF-κB in both cell types. Consistent with this, treatment of a NF-κB/Jurkat/GFP^{TM} Transcriptional Reporter Cell Line with increasing concentrations of NaHS did not lead to increased green fluorescent protein expression, indicating no change in transcriptional activity (Fig. 7b). Mass cytometry analysis of PBMCs stimulated with NaHS (1 mM), TNFα (20 ng/ml) or LPS (1 μg/ml) for ten minutes revealed similar signaling responses, with no change in p-NF-κB induced by NaHS in all subsets (CD4 T-cells, naive CD8 T-cells, memory CD8 T-cells, NK-cells, and both subsets of monocytes) (Fig. 7c-d).

4. Discussion

The actual level of physiological concentrations of H_2S *in vivo* has been difficult to determine and may have been overestimated due to limitations in the methodologies applied [61,62]. The widely used methylene blue assay measures acid-labile sulphur in addition to free sulfide in plasma in the μM range [63], while newer techniques measure free sulfide and soluble gas in

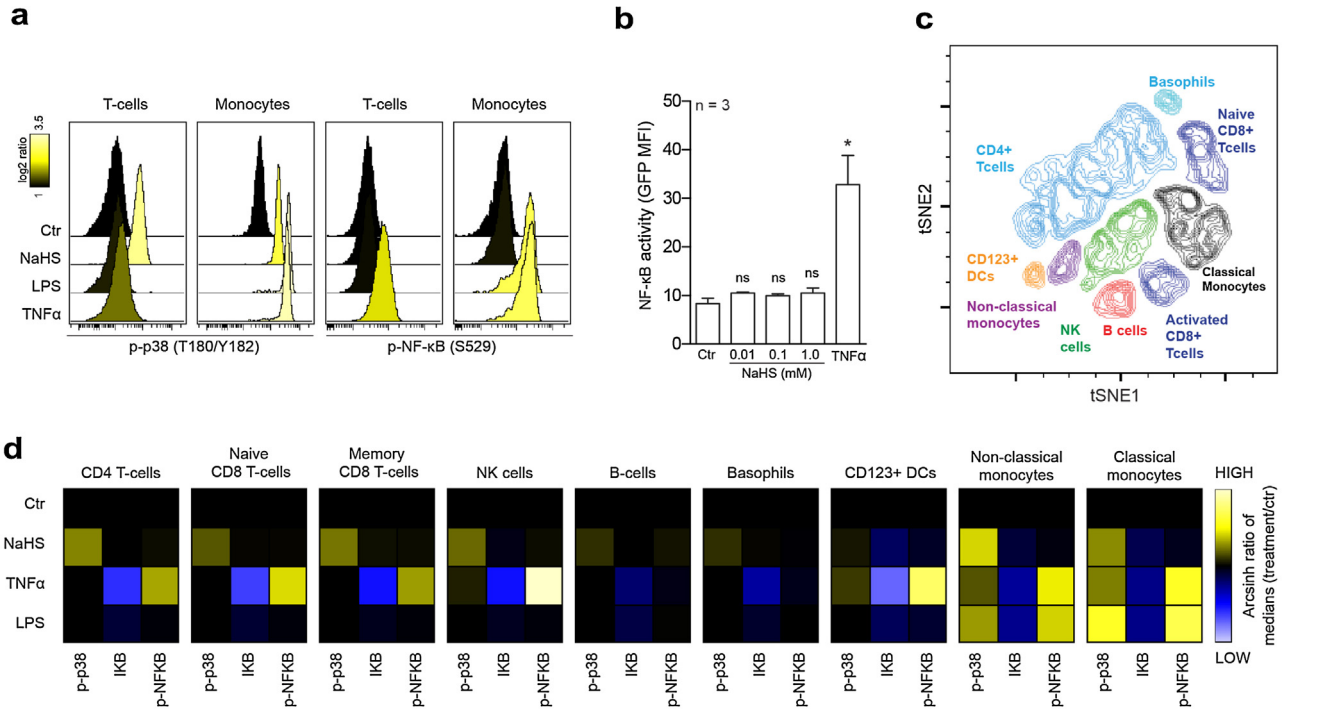

Fig. 7. *In vitro* treatment of PBMCs with sodium hydrosulfide does not modulate p-NF-κB. (a) Histogram overlay displays median log2 ratio of p-p38 T180/Y182 and p-NF-κB in T-cells and monocytes stimulated with NaHS (1 mM, 10 min), LPS (1.0 μg/ml, 10 min) or TNFα (20 ng/ml, 10 min). Vehicle treated cells were used as control. (b) Plot displaying GFP median fluorescent intensities of the NF-κB/Jurkat/GFP^{TM} Transcriptional Reporter Cell Line treated with NaHS or TNFα (0.25 ng/ml) and incubated for 24 h. Student's paired *t*-tests were conducted to compare MFI in treated groups with the control groups ($^{*}p \leq 0.05$, ns $p > 0.05$). (c) Bivariate viSNE contour plot displaying identified subsets of PBMCs; CD4 T-cells ($CD3^{+}CD4^{+}$), CD8 T-cells ($CD3^{+}CD8^{+}$), B-cells ($CD19^{+}CD20^{+}HLA\text{-}DR^{+}$), NK cells ($CD16^{+}HLA\text{-}DR^{-}$), Basophils ($CD123^{+}CD11c^{+}$), $CD123^{+}$ DCs ($CD123^{+}CD11c^{-}$), non-classical monocytes ($HLA\text{-}DR^{+}CD16^{+}$) and classical monocytes ($HLA\text{-}DR^{+}CD14^{+}$). All viSNE plots displaying expression of phenotypic markers individually are available in Supplemental Fig. S7. (d) Heat maps displaying the arcsinh change, relative to vehicle treated control, of the median metal intensity (MMI) of p-p38 (T180/Y182), p-NF-κB (S529) and IκB in subsets of PBMCs identified in (c).

the nM range [8,9]. It has been pointed out that most studies have reported biological effects of H_2S in the 10–100 μM range [64], this is in line with the present study where a concentration-response relationship between NaHS and p-p38 is detected at 10–1000 μM in PBMCs (Fig. 1f). Another sulphur molecule, sodium thiosulphate ($Na_2S_2O_3$), is used therapeutically in millimolar serum concentration against calcific uremic arteriolopathy, also known as calciphylaxis [65]. However, the concentrations of free sulfide in plasma from healthy individuals and patients with cardiovascular disease have been determined to be <1 μM [8,12]. Therefore, signaling described in the present study is likely detected at supra-physiological concentrations of H_2S. However, it has been proposed that the concentration of H_2S in inflammatory micro milieu like synovial fluid of rheumatoid arthritis patients exceeds what is measured in blood [13]. This has been determined with the methylene blue assay, and it is unknown whether these concentrations are reflecting free sulfide, acid-labile sulfide or both [13]. The use of techniques that precisely determine free sulfide levels could aid in determining whether the signaling described in the present study is relevant for immune cells in synovial fluid in patients with rheumatoid arthritis. However, the lower supra-physiological concentrations of sulfide used in the present study could be relevant during environmental or occupational exposure to higher than ambient concentrations of H_2S [50]. For comparison, the equivalent plasma sulfide concentration during atmospheric exposure of 20 ppm H_2S has been estimated equal to 6.5 μM [15].

The discussion about physiological relevance for various concentrations of H_2S is also complicated by the presence of polysulfides (H_2S_n) formed by many of the sodium salts used to study this gas *in vitro* [66]. Concentrations of H_2S in solutions of NaHS are therefore lower than estimated, and polysulfides could in fact be the active agent. Polysulfides are also generated when making sulfide solutions from H_2S gas, implying that studying H_2S separately from polysulfides is practically impossible [66]. Studies in astrocytes have shown that polysulfides activate a calcium influx in these cells through opening of transient receptor potential (TRP) channels at substantial lower concentrations (EC_{50} 91 nM) compared to what NaHS does (EC_{50} 116 μM) [43,67]. Endogenous polysulfides have been detected in HeLa cells [68], zebra fish [68] and brain tissue of rats [67], and have been suggested to be endogenous H_2S-derived signaling molecules that modify thiol groups of cysteines in proteins [66,69]. It is therefore possible that signaling described in the present study is mediated by nM range concentrations of polysulfides.

This study describes NaHS-induced signaling of p38 with Akt and CREB/ATF1 as partial and complete downstream proteins, respectively (Figs. 1, 5 and 6). Interestingly, classical monocytes displayed a lacking property to down-regulate the signaling compared to lymphocytes. H_2S is known to inactivate phosphatases through sulfhydration [70], and this could indicate that classical monocytes are particularly prone to such inactivation and thereby susceptible to long-term influence by sulfides. Activation of p38 is known to increase COX-2 expression in these cells [71]. Inhibition of endogenous H_2S synthesis attenuates COX-2 transcription and prostaglandin production in a colitis rat model [21], and exogenous H_2S has also been described to increase COX-2 expression [72]. Treatment of macrophages with NaSH (100–200 μM) in combination with LPS does result in reduced release of PGE_2 [2].

NF-κB p65 is essential in mounting a cytokine response after proinflammatory stimuli [23], and its activity is modulated by H_2S [2,31]. However, the stimulation with NaHS alone did not lead to activation of NF-κB p65 (Fig. 7). Whiteman et al. showed that com-

bination treatment with NaHS and LPS increased NF-κB p65 activity and secretion of TNFα and IL-1β compared to LPS treatment alone [2]. In light of the signaling described in the present study, this could be due to partly overlapping signal transduction induced by LPS and NaHS. The lack of NF-κB transcriptional activation in the present study is in line with a study where stimulation with NaHS alone did not influence cytokine production in immune cells [1]. The stress kinase p38 is often referred to as being important in the pro-inflammatory cytokine response, however, such studies often investigate p38 in the context of activated NF-κB [28]. Activation of p38 is also known to increase expression of the anti-inflammatory cytokine IL-10 [30], and therapeutic inhibition of p38 in rheumatoid arthritis patients has so far been disappointing, suggesting that this protein is not pivotal in this inflammatory disease [73]. In this light, it could be that activated p38 by NaHS could actually have mostly anti-inflammatory repercussions. Phosphorylation and activation of Akt by H_2S is suggested to lead to survival and angiogenesis in vascular smooth muscle cells [46] and endothelial cells [48], respectively. Functional effects of NaHS-induced Akt activation in PBMCs have not been elaborated. However, Akt1 ablation in mice has been shown to lead to differentiation of macrophages towards an M1 type [74], and increased activity of the PI3K-Akt-mTOR pathway leads to differentiation of human monocytes towards an M2 type [49]. The latter is considered anti-inflammatory; they produce less nitric oxide and are involved in tissue repair and resolution of inflammation [75]. Interestingly, mice treated with NaHS prior to myocardial infarction are reported to exhibit enhanced M2 differentiation of macrophages in cardiac tissues [76]. Our observation of NaHS-induced sustained phosphorylation of Akt in monocytes provided in the present study could indicate a macrophage differentiation effect also in human tissue.

To investigate the molecular mechanism of the signaling induced by NaHS, the highest concentration used in the present study (1 mM) was chosen to achieve a clear phosphorylation effect suitable for combination studies to evaluate preventive effect of pharmacological inhibitors or calcium chelators. H_2S has been reported to influence several processes that could be relevant for p38; cyclic nucleotide signaling [77], ion channel function [78], tyrosine phosphatase activity [79] and PKC activity [41]. Experiments were carried out in PBMCs or Jurkat cells where pharmacological inhibition of these processes was investigated for potential effect on NaHS-induced phosphorylation of p38 (Figs. 2-4). Notably, chelation of intracellular calcium and inhibitors of p38 and Hsp90 attenuated the phosphorylation of p38 induced by NaHS (Figs. 2 and 4). Autophosphorylation of p38 have been described to take place during noncanonical p38 activation, which occurs by destabilization of an Hsp90-Cdc37-p38 complex [80]. Due to the strong ability of p38 and Hsp90 inhibitors to attenuate the effect of NaHS, it is possible that H_2S induces p38 phosphorylation through such noncanonical activation by sulfhydration of this complex, followed by p38 autophosphorylation. Further evaluation of possible sulfhydration of cysteines in Hsp90, Cdc37 or p38 itself may identify a more precise mechanism of NaHS-induced phosphorylation of p38. The absent effect of the geldanamycin analog 17-AAG in our assay (Fig. 4a) is consistent with a previous report where 17-AAG was a weaker p38-activator compared to geldanamycin [80]. Chelation of intracellular calcium attenuated the phosphorylation of both p38 (Fig. 2e) and Akt (Fig. 5h). Interestingly, BAPTA-AM treatment is reported to modulate the architecture of Hsp90 protein complexes [81], and both p38 and Akt is known to form complexes with Hsp90 [80,82]. Preincubation with BAPTA-AM could therefore possibly reorganize the protein complexes in such a way that NaHS no longer leads to activation of signaling. This is in accordance with Akt phosphorylation being only partly dependent on p38-Akt crosstalk (Fig. 5a-c). However, the Akt phosphorylation may also be due to inactivated phosphatase and tensin homolog (PTEN) by NaSH [66].

Most inhibitors of PKC did not alter the effect of NaHS on p38, except for chelerythrine, which alone induced phosphorylation of p38, possibly masking the effect of NaHS (Fig. 3d). This is supported by the fact that chelerythrine is also known to activate p38 through an unknown PKC-independent mechanism [83]. Based on this and the lacking effect of the other PKC inhibitors used, we consider it unlikely that activation of PKC caused p38 phosphorylation induced by NaHS in PBMCs. Chelating extracellular calcium with EGTA or BAPTA (Fig. 2a-c, e), or inhibiting IP3R, calmodulin or CaMKII (Fig. 3a–c) did not prevent signaling induced by NaHS. This indicates that phosphorylation of p38 by NaHS is not a downstream effect of calcium influx, calcium release from the ER or calmodulin dependent signaling. H_2S can also induce inhibition of mitochondrial respiration [57], and this may be sensed by the metabolic switch AMP-activated protein kinase (AMPK) upstream of p38 [84]. No significant reduction in concentration of ATP in PBMCs was detected upon stimulation with NaHS. The highest concentration NaHS did show a clear non-significant reduction in ATP, but phosphorylation of p38 was induced at lower concentrations. Also, sulfide-induced phosphorylation of p38 is reported to be dependent on K_{ATP} channels in endothelial cells [35], however, NaSH-induced p-p38 was not attenuated by glibenclamide in the present study (Fig. 4a).

In conclusion, NaHS induces concentration-dependent signaling with p38, Akt and CREB/ATF1 involved in human PBMCs. Reduced effect of NaHS by intracellular calcium chelation and inhibitors targeting p38 and Hsp90 suggest that the mechanism of activation could be through non-canonical activation of p38. Future studies should investigate possible targets of sulfhydration and address if H_2S or derived polysulfides functionally influence differentiation of monocytes towards an anti-inflammatory macrophage subset.

Authors contributions

BTG and AS designed and planned the study. AS conducted *in vitro* experiments and flow cytometry analyzes. AS, SG, LB, JS and SG conducted the mass cytometry analysis. AS performed the statistical analyzes. DM carried out the automated small molecule inhibitor phosphoflow screen. BTG and AS wrote the manuscript. All authors read, edited and approved the final manuscript. The authors declare no conflict of interest.

Funding

This study was performed with funding from the The Research Council of Norway (Petromaks program grant #220759).

Acknowledgments

We are thankful for Bergen Research Foundation and their support to the University of Bergen for the mass cytometer equipment used in this study. We also thank Dr. Vibeke Andresen for valuable discussions and Samantha Scarlett for proofreading the manuscript.

Appendix A. Supplementary data

Supplementary data associated with this article can be found, in the online version, at http://dx.doi.org/10.1016/j.phrs.2016.08.018.

References

[1] N. Dufton, J. Natividad, E.F. Verdu, J.L. Wallace, Hydrogen sulfide and resolution of acute inflammation: a comparative study utilizing a novel fluorescent probe, Sci. Rep. 2 (2012) 499.
[2] M. Whiteman, L. Li, P. Rose, C.H. Tan, D.B. Parkinson, P.K. Moore, The effect of hydrogen sulfide donors on lipopolysaccharide-induced formation of

inflammatory mediators in macrophages, Antioxid. Redox Signal. 12 (2010) 1147–1154.
[3] M. Whiteman, P.G. Winyard, Hydrogen sulfide and inflammation: the good, the bad, the ugly and the promising, Expert Rev. Clin. Pharmacol. 4 (2011) 13–32.
[4] C. Coletta, K. Modis, B. Szczesny, A. Brunyanszki, G. Olah, E.C. Rios, K. Yanagi, A. Ahmad, A. Papapetropoulos, C. Szabo, Regulation of vascular tone, angiogenesis and cellular bioenergetics by the 3-mercaptopyruvate sulfurtransferase/H2S pathway: functional impairment by hyperglycemia and restoration by DL-alpha-lipoic acid, Mol. Med. 21 (2015) 1–14.
[5] T. Chiku, D. Padovani, W.D. Zhu, S. Singh, V. Vitvitsky, R. Banerjee, H2S biogenesis by human cystathionine gamma-lyase leads to the novel sulfur metabolites lanthionine and homolanthionine and is responsive to the grade of hyperhomocysteinemia, J. Biol. Chem. 284 (2009) 11601–11612.
[6] S. Singh, D. Padovani, R.A. Leslie, T. Chiku, R. Banerjee, Relative contributions of cystathionine beta-synthase and gamma-cystathionase to H2S biogenesis via alternative trans-sulfuration reactions, J. Biol. Chem. 284 (2009) 22457–22466.
[7] N. Shibuya, Y. Mikami, Y. Kimura, N. Nagahara, H. Kimura, Vascular endothelium expresses 3-mercaptopyruvate sulfurtransferase and produces hydrogen sulfide, J. Biochem. 146 (2009) 623–626.
[8] X. Shen, E.A. Peter, S. Bir, R. Wang, C.G. Kevil, Analytical measurement of discrete hydrogen sulfide pools in biological specimens, Free Radic. Biol. Med. 52 (2012) 2276–2283.
[9] N.L. Whitfield, E.L. Kreimier, F.C. Verdial, N. Skovgaard, K.R. Olson, Reappraisal of H2S/sulfide concentration in vertebrate blood and its potential significance in ischemic preconditioning and vascular signaling, Am. J. Physiol. Regul. Integr. Comp. Physiol. 294 (2008) R1930–R1937.
[10] L. Li, M. Bhatia, Y.Z. Zhu, Y.C. Zhu, R.D. Ramnath, Z.J. Wang, F.B.M. Anuar, M. Whiteman, M. Salto-Tellez, P.K. Moore, Hydrogen sulfide is a novel mediator of lipopolysaccharide-induced inflammation in the mouse, FASEB J. 19 (2005) 1196–1198.
[11] Y.Y. Mok, M.S. Atan, C. Yoke Ping, W. Zhong Jing, M. Bhatia, S. Moochhala, P.K. Moore, Role of hydrogen sulphide in haemorrhagic shock in the rat: protective effect of inhibitors of hydrogen sulphide biosynthesis, Br. J. Pharmacol. 143 (2004) 881–889.
[12] E.A. Peter, X. Shen, S.H. Shah, S. Pardue, J.D. Glawe, W.W. Zhang, P. Reddy, N.I. Akkus, J. Varma, C.G. Kevil, Plasma free H2S levels are elevated in patients with cardiovascular disease, J. Am. Heart Assoc. 2 (2013) e000387.
[13] M. Whiteman, R. Haigh, J.M. Tarr, K.M. Gooding, A.C. Shore, P.G. Winyard, Detection of hydrogen sulfide in plasma and knee-joint synovial fluid from rheumatoid arthritis patients: relation to clinical and laboratory measures of inflammation, Ann. N.Y. Acad. Sci. 1203 (2010) 146–150.
[14] N. Muniraj, L.K. Stamp, A. Badiei, A. Hegde, V. Cameron, M. Bhatia, Hydrogen sulfide acts as a pro-inflammatory mediator in rheumatic disease, Int. J. Rheum. Dis. (2014).
[15] K.R. Olson, The therapeutic potential of hydrogen sulfide: separating hype from hope, Am. J. Physiol. Regul. Integr. Comp. Physiol. 301 (2011) R297–312.
[16] J.L. Wallace, R. Wang, Hydrogen sulfide-based therapeutics: exploiting a unique but ubiquitous gasotransmitter, Nat. Rev. Drug Discov. 14 (2015) 329–345.
[17] E. Ekundi-Valentim, K.T. Santos, E.A. Camargo, A. Denadai-Souza, S.A. Teixeira, C.I. Zanoni, A.D. Grant, J. Wallace, M.N. Muscara, S.K. Costa, Differing effects of exogenous and endogenous hydrogen sulphide in carrageenan-induced knee joint synovitis in the rat, Br. J. Pharmacol. 159 (2010) 1463–1474.
[18] S. Fiorucci, E. Antonelli, E. Distrutti, G. Rizzo, A. Mencarelli, S. Orlandi, R. Zanardo, B. Renga, M. Di Sante, A. Morelli, G. Cirino, J.L. Wallace, Inhibition of hydrogen sulfide generation contributes to gastric injury caused by anti-inflammatory nonsteroidal drugs, Gastroenterology 129 (2005) 1210–1224.
[19] I. Hirata, Y. Naito, T. Takagi, K. Mizushima, T. Suzuki, T. Omatsu, O. Handa, H. Ichikawa, H. Ueda, T. Yoshikawa, Endogenous hydrogen sulfide is an anti-inflammatory molecule in dextran sodium sulfate-induced colitis in mice, Digest. Dis. Sci. 56 (2011) 1379–1386.
[20] J.L. Wallace, M. Dicay, W. McKnight, G.R. Martin, Hydrogen sulfide enhances ulcer healing in rats, FASEB J. 21 (2007) 4070–4076.
[21] J.L. Wallace, L. Vong, W. McKnight, M. Dicay, G.R. Martin, Endogenous and exogenous hydrogen sulfide promotes resolution of colitis in rats, Gastroenterology 137 (2009) 569–578.
[22] P.P. Tak, G.S. Firestein, NF-kappaB. a key role in inflammatory diseases, J. Clin. Invest. 107 (2001) 7–11.
[23] U.J. Lee, S.R. Choung, K.V.B. Prakash, E.J. Lee, M.Y. Lee, Y.J. Kim, C.W. Han, Y.C. Chol, Dual knockdown of p65 and p50 subunits of NF-kappaB by siRNA inhibits the induction of inflammatory cytokines and significantly enhance apoptosis in human primary synoviocytes treated with tumor necrosis factor-alpha, Mol. Biol. Rep. 35 (2008) 291–298.
[24] A. Banerjee, S. Gerondakis, Coordinating TLR-activated signaling pathways in cells of the immune system, Immunol. Cell Biol. 85 (2007) 420–424.
[25] D. Brenner, H. Blaser, T.W. Mak, Regulation of tumour necrosis factor signalling: live or let die, Nat. Rev. Immunol. 15 (2015) 362–374.
[26] Z. Guan, S.Y. Buckman, A.P. Pentland, D.J. Templeton, A.R. Morrison, Induction of cyclooxygenase-2 by the activated MEKK1 –> SEK1/MKK4 –> p38 mitogen-activated protein kinase pathway, J. Biol. Chem. 273 (1998) 12901–12908.
[27] D.G. Perregaux, D. Dean, M. Cronan, P. Connelly, C.A. Gabel, Inhibition of interleukin-1 beta production by SKF86002: evidence of two sites of in vitro activity and of a time and system dependence, Mol. Pharmacol. 48 (1995) 433–442.
[28] T. Tomida, M. Takekawa, H. Saito, Oscillation of p38 activity controls efficient pro-inflammatory gene expression, Nat. Commun. 6 (2015) 8350.
[29] C. Chen, Y.H. Chen, W.W. Lin, Involvement of p38 mitogen-activated protein kinase in lipopolysaccharide-induced iNOS and COX-2 expression in J774 macrophages, Immunology 97 (1999) 124–129.
[30] K. Gee, J.B. Angel, S. Mishra, M.A. Blahoianu, A. Kumar, IL-10 regulation by HIV-Tat in primary human monocytic cells: involvement of calmodulin/calmodulin-dependent protein kinase-activated p38 MAPK and Sp-1 and CREB-1 transcription factors, J. Immunol. 178 (2007) 798–807.
[31] N. Sen, B.D. Paul, M.M. Gadalla, A.K. Mustafa, T. Sen, R.S. Xu, S. Kim, S.H. Snyder, Hydrogen sulfide-linked sulfhydration of NF-kappa B mediates its antiapoptotic actions, Mol. Cell. 45 (2012) 13–24.
[32] J. Du, Y. Huang, H. Yan, Q. Zhang, M. Zhao, M. Zhu, J. Liu, S.X. Chen, D. Bu, C. Tang, H. Jin, Hydrogen sulfide suppresses oxidized low-density lipoprotein (ox-LDL)-stimulated monocyte chemoattractant protein 1 generation from macrophages via the nuclear factor kappaB (NF-kappaB) pathway, J. Biol. Chem. 289 (2014) 9741–9753.
[33] G. Yang, W. Yang, L. Wu, R. Wang, H2S, endoplasmic reticulum stress, and apoptosis of insulin-secreting beta cells, J. Biol. Chem. 282 (2007) 16567–16576.
[34] G. Yang, X. Sun, R. Wang, Hydrogen sulfide-induced apoptosis of human aorta smooth muscle cells via the activation of mitogen-activated protein kinases and caspase-3, FASEB J. 18 (2004) 1782–1784.
[35] A. Papapetropoulos, A. Pyriochou, Z. Altaany, G.D. Yang, A. Marazioti, Z.M. Zhou, M.G. Jeschke, L.K. Branski, D.N. Herndon, R. Wang, C. Szabo, Hydrogen sulfide is an endogenous stimulator of angiogenesis, Proc. Natl. Acad. Sci. U. S. A. 106 (2009) 21972–21977.
[36] L. Zhao, Y. Wang, Q. Yan, W. Lv, Y. Zhang, S. He, Exogenous hydrogen sulfide exhibits anti-cancer effects though p38 MAPK signaling pathway in C6 glioma cells, Biol. Chem. 396 (2015) 1247–1253.
[37] L. Rinaldi, G. Gobbi, M. Pambianco, C. Micheloni, P. Mirandola, M. Vitale, Hydrogen sulfide prevents apoptosis of human PMN via inhibition of p38 and caspase 3, Lab. Invest. 86 (2006) 391–397.
[38] H. Enslen, H. Tokumitsu, P.J. Stork, R.J. Davis, T.R. Soderling, Regulation of mitogen-activated protein kinases by a calcium/calmodulin-dependent protein kinase cascade, Proc. Natl. Acad. Sci. U. S. A. 93 (1996) 10803–10808.
[39] K. Takeda, A. Matsuzawa, H. Nishitoh, K. Tobiume, S. Kishida, J. Ninomiya-Tsuji, K. Matsumoto, H. Ichijo, Involvement of ASK1 in Ca2+-induced p38 MAP kinase activation, EMBO Rep. 5 (2004) 161–166.
[40] K. Nakajima, Y. Tohyama, S. Kohsaka, T. Kurihara, Protein kinase C alpha requirement in the activation of p38 mitogen-activated protein kinase, which is linked to the induction of tumor necrosis factor alpha in lipopolysaccharide-stimulated microglia, Neurochem. Int. 44 (2004) 205–214.
[41] T.T. Pan, K.L. Neo, L.F. Hu, Q.C. Yong, J.S. Bian, H2S preconditioning-induced PKC activation regulates intracellular calcium handling in rat cardiomyocytes, Am. J. Physiol. Cell Physiol. 294 (2008) C169–177.
[42] S.F. Steinberg, Structural basis of protein kinase C isoform function, Physiol. Rev. 88 (2008) 1341–1378.
[43] Y. Nagai, M. Tsugane, J. Oka, H. Kimura, Hydrogen sulfide induces calcium waves in astrocytes, FASEB J. 18 (2004) 557–559.
[44] V.A. McGuire, A. Gray, C.E. Monk, S.G. Santos, K. Lee, A. Aubareda, J. Crowe, N. Ronkina, J. Schwermann, I.H. Batty, N.R. Leslie, J.L. Dean, S.J. O'Keefe, M. Boothby, M. Gaestel, J.S. Arthur, Cross talk between the Akt and p38alpha pathways in macrophages downstream of Toll-like receptor signaling, Mol. Cell Biol. 33 (2013) 4152–4165.
[45] M.J. Rane, P.Y. Coxon, D.W. Powell, R. Webster, J.B. Klein, W. Pierce, P. Ping, K.R. McLeish, p38 Kinase-dependent MAPKAPK-2 activation functions as 3-phosphoinositide-dependent kinase-2 for Akt in human neutrophils, J. Biol. Chem. 276 (2001) 3517–3523.
[46] Y. Zhou, D. Wang, X. Gao, K. Lew, A.M. Richards, P. Wang, mTORC2 phosphorylation of Akt1: a possible mechanism for hydrogen sulfide-induced cardioprotection, PLoS One 9 (2014) e99665.
[47] R. Tamizhselvi, J. Sun, Y.H. Koh, M. Bhatia, Effect of hydrogen sulfide on the phosphatidylinositol 3-kinase-protein kinase B pathway and on caerulein-induced cytokine production in isolated mouse pancreatic acinar cells, J. Pharmacol. Exp. Ther. 329 (2009) 1166–1177.
[48] Z. Altaany, G.D. Yang, R. Wang, Crosstalk between hydrogen sulfide and nitric oxide in endothelial cells, J. Cell Mol. Med. 17 (2013) 879–888.
[49] C. Rocher, D.K. Singla, SMAD-PI3K-Akt-mTOR pathway mediates BMP-7 polarization of monocytes into M2 macrophages, PLoS One 8 (2013).
[50] A. Sulen, S.H. Lygre, S.M. Hjelle, B.E. Hollund, B.T. Gjertsen, Elevated monocyte phosphorylated p38 in nearby employees after a chemical explosion, Sci. Rep. 6 (2016) 29060.
[51] B. Bodenmiller, E.R. Zunder, R. Finck, T.J. Chen, E.S. Savig, R.V. Bruggner, E.F. Simonds, S.C. Bendall, K. Sachs, P.O. Krutzik, G.P. Nolan, Multiplexed mass cytometry profiling of cellular states perturbed by small-molecule regulators, Nat. Biotechnol. 30 (2012) 858–867.
[52] J.M. Irish, D.K. Czerwinski, G.P. Nolan, R. Levy, Altered B-cell receptor signaling kinetics distinguish human follicular lymphoma B cells from tumor-infiltrating nonmalignant B cells, Blood 108 (2006) 3135–3142.
[53] S. Gavasso, S.E. Gullaksen, J. Skavland, B.T. Gjertsen, Single-cell proteomics: potential implications for cancer diagnostics, Expert Rev. Mol. Daign. (2016) 1–11.

[54] P.O. Krutzik, G.P. Nolan, Fluorescent cell barcoding in flow cytometry allows high-throughput drug screening and signaling profiling, Nat. Methods 3 (2006) 361–368.
[55] J. Skavland, K.M. Jorgensen, K. Hadziavdic, R. Hovland, I. Jonassen, O. Bruserud, B.T. Gjertsen, Specific cellular signal-transduction responses to in vivo combination therapy with ATRA, valproic acid and theophylline in acute myeloid leukemia, Blood Cancer J. 1 (2011) e4.
[56] A.D. Amir el, K.L. Davis, M.D. Tadmor, E.F. Simonds, J.H. Levine, S.C. Bendall, D.K. Shenfeld, S. Krishnaswamy, G.P. Nolan, D. Pe'er, viSNE enables visualization of high dimensional single-cell data and reveals phenotypic heterogeneity of leukemia, Nat. Biotechnol. 31 (2013) 545–552.
[57] C. Szabo, C. Ransy, K. Modis, M. Andriamihaja, B. Murghes, C. Coletta, G. Olah, K. Yanagi, F. Bouillaud, Regulation of mitochondrial bioenergetic function by hydrogen sulfide: part I. Biochemical and physiological mechanisms, Br. J. Pharmacol. 171 (2014) 2099–2122.
[58] K. Mikoshiba, M. Hattori, IP3 receptor-operated calcium entry, Sci. Signal. 2000 (2000) pe1.
[59] E. Hosoi, C. Nishizaki, K.L. Gallagher, H.W. Wyre, Y. Matsuo, Y. Sei, Expression of the ryanodine receptor isoforms in immune cells, J. Immunol. 167 (2001) 4887–4894.
[60] J.T. Lanner, D.K. Georgiou, A.D. Joshi, S.L. Hamilton, Ryanodine receptors: structure, expression, molecular details, and function in calcium release, Cold Spring Harb. Perspect. Biol. 2 (2010) a003996.
[61] J. Furne, A. Saeed, M.D. Levitt, Whole tissue hydrogen sulfide concentrations are orders of magnitude lower than presently accepted values, Am. J. Physiol. Regul. Integr. Comp. Physiol. 295 (2008) R1479–1485.
[62] K.R. Olson, Is hydrogen sulfide a circulating gasotransmitter in vertebrate blood? BBA-Bioenergetics 1787 (2009) 856–863.
[63] G.K. Kolluru, X. Shen, S.C. Bir, C.G. Kevil, Hydrogen sulfide chemical biology: pathophysiological roles and detection, Nitric Oxide 35 (2013) 5–20.
[64] O. Kabil, R. Banerjee, Redox biochemistry of hydrogen sulfide, J. Biol. Chem. 285 (2010) 21903–21907.
[65] S.U. Nigwekar, D. Kroshinsky, R.M. Nazarian, J. Goverman, R. Malhotra, V.A. Jackson, M.M. Kamdar, D.J. Steele, R.I. Thadhani, Calciphylaxis: risk factors, diagnosis, and treatment, Am. J. Kidney Dis. 66 (2015) 133–146.
[66] R. Greiner, Z. Palinkas, K. Basell, D. Becher, H. Antelmann, P. Nagy, T.P. Dick, Polysulfides link H2S to protein thiol oxidation, Antioxid. Redox Signal. 19 (2013) 1749–1765.
[67] Y. Kimura, Y. Mikami, K. Osumi, M. Tsugane, J. Oka, H. Kimura, Polysulfides are possible H2S-derived signaling molecules in rat brain, FASEB J. 27 (2013) 2451–2457.
[68] L. Zeng, S. Chen, T. Xia, W. Hu, C. Li, Z. Liu, Two-photon fluorescent probe for detection of exogenous and endogenous hydrogen persulfide and polysulfide in living organisms, Anal. Chem. 87 (2015) 3004–3010.
[69] H. Kimura, Signaling molecules: hydrogen sulfide and polysulfide, Antioxid. Redox Signal. 22 (2015) 362–376.
[70] N. Krishnan, C. Fu, D.J. Pappin, N.K. Tonks, H2S-Induced sulfhydration of the phosphatase PTP1B and its role in the endoplasmic reticulum stress response, Sci. Signal. 4 (2011) ra86.
[71] J.L. Dean, M. Brook, A.R. Clark, J. Saklatvala, p38 mitogen-activated protein kinase regulates cyclooxygenase-2 mRNA stability and transcription in lipopolysaccharide-treated human monocytes, J. Biol. Chem. 274 (1999) 264–269.
[72] S.F. Ang, S.W. Sio, S.M. Moochhala, P.A. MacAry, M. Bhatia, Hydrogen sulfide upregulates cyclooxygenase-2 and prostaglandin E metabolite in sepsis-evoked acute lung injury via transient receptor potential vanilloid type 1 channel activation, J. Immunol. 187 (2011) 4778–4787.
[73] D. Hammaker, G.S. Firestein, Go upstream, young man: lessons learned from the p38 saga, Ann. Rheum. Dis. 69 (Suppl. 1) (2010) i77–82.
[74] A. Arranz, C. Doxaki, E. Vergadi, Y. Martinez de la Torre, K. Vaporidi, E.D. Lagoudaki, E. Ieronymaki, A. Androulidaki, M. Venihaki, A.N. Margioris, E.N. Stathopoulos, P.N. Tsichlis, C. Tsatsanis, Akt1 and Akt2 protein kinases differentially contribute to macrophage polarization, Proc. Natl. Acad. Sci. U. S. A. 109 (2012) 9517–9522.
[75] P. Italiani, D. Boraschi, From monocytes to M1/M2 macrophages: phenotypical vs: functional differentiation, Front. Immunol. 5 (2014) 514.
[76] L. Miao, X. Shen, M. Whiteman, H. Xin, Y. Shen, X. Xin, P.K. Moore, Y.Z. Zhu, Hydrogen sulfide mitigates myocardial infarction via promotion of mitochondrial biogenesis-dependent m2 polarization of macrophages, Antioxid. Redox Signal. 25 (2016) 268–281.
[77] M. Bucci, A. Papapetropoulos, V. Vellecco, Z.M. Zhou, A. Pyriochou, C. Roussos, F. Roviezzo, V. Brancaleone, G. Cirino, Hydrogen sulfide is an endogenous inhibitor of phosphodiesterase activity, Arterioscl. Throm. Vas. 30 (2010) 1998–2004.
[78] R. Wang, Physiological implications of hydrogen sulfide: a whiff exploration that blossomed, Physiol. Rev. 92 (2012) 791–896.
[79] P. Heneberg, Reactive nitrogen species and hydrogen sulfide as regulators of protein tyrosine phosphatase activity, Antioxid. Redox Sign. 20 (2014) 2191–2209.
[80] A. Ota, J. Zhang, P.P. Ping, J.H. Han, Y.B. Wang, Specific regulation of noncanonical p38 alpha activation by Hsp90-Cdc37 chaperone complex in cardiomyocyte, Circ. Res. 106 (2010) 1404–1412.
[81] S. Takahashi, M.E. Mendelsohn, Synergistic activation of endothelial nitric-oxide synthase (eNOS) by HSP90 and Akt: calcium-independent eNOS activation involves formation of an HSP90-Akt-CaM-bound eNOS complex, J. Biol. Chem. 278 (2003) 30821–30827.
[82] O. Franzese, S.M. Henson, C. Naro, E. Bonmassar, Defect in HSP90 expression in highly differentiated human CD8(+) T lymphocytes, Cell. Death. Dis. 5 (2014) e1294.
[83] R. Yu, S. Mandlekar, T.H. Tan, A.N. Kong, Activation of p38 and c-Jun N-terminal kinase pathways and induction of apoptosis by chelerythrine do not require inhibition of protein kinase C, J. Biol. Chem. 275 (2000) 9612–9619.
[84] J. Li, E.J. Miller, J. Ninomiya-Tsuji, R.R. Russell, 3rd, Young LH. AMP-activated protein kinase activates p38 mitogen-activated protein kinase by increasing recruitment of p38 MAPK to TAB1 in the ischemic heart, Circ. Res. 97 (2005) 872–879.